

X-ray Observations of BL Lacertae During 1997 Outburst and its Association with Quasar-like Characteristics

Greg M. Madejski^{1,2}, Marek Sikora³, Tess Jaffe^{1,4}, Michał Błażejowski³, Keith Jahoda¹, &
Rafał Moderski^{3,5}

¹Lab for High Energy Astrophysics, NASA/Goddard, Greenbelt, MD 20771

²also with the Dept. of Astronomy, Univ. of Maryland, College Park;

³Copernicus Astronomical Center, Bartycka 18, 00-716 Warsaw, Poland;

⁴also with Raytheon STX;

⁵JILA, University of Colorado, Campus Box 440, Boulder, CO 80309

Received _____; accepted _____

ABSTRACT

This paper reports on the X-ray emission from BL Lacertae during its July 1997 outburst as observed with the Rossi X-ray Timing Explorer (RXTE), compares the RXTE data to previous measurements, and interprets the overall electromagnetic emission in the context of the currently popular theoretical models. The source is bright and variable, with the 2 – 10 keV flux approximately two to three and a half times higher than measured in November 1995 by *Asca*. The spectrum is also harder, with power law energy indices of $\sim 0.4 - 0.6$, compared to ~ 0.9 in Nov. 1995. Both in the optical band, where BL Lacertae now shows broad emission lines, and in the X-ray band, where the spectrum is hard, the overall electromagnetic distribution of BL Lacertae is similar to that observed in blazars associated with quasars rather than to that seen in the more common High-energy - peaked BL Lac - type objects (HBLs). We argue that the high energy (X-ray and γ -ray) emission from BL Lacertae consists of two spectral components: X-rays are produced by Comptonization of synchrotron radiation, while the γ -rays produced by Comptonization of the broad emission line flux.

Subject headings: X-rays: observations – galaxies: active – quasars: BL Lacertae – theory: radiation mechanisms

1. INTRODUCTION

The eponymous BL Lacertae has been identified as a counterpart of the variable radio source VRO 42.22.01 by Schmitt (1968); subsequent work by Oke, Neugebauer, & Becklin (1969) as well as DuPuy *et al.*(1969) revealed a featureless spectrum, devoid of emission or absorption lines. In 1972, Strittmatter *et al.*(1972) suggested that BL Lac-type objects are akin to Quasi-Stellar Radio Sources, but distinguished by the absence of emission lines. Detailed spectroscopy of BL Lacertae by Miller & Hawley (1977) revealed an absorption line system at a redshift of 0.069, presumably due to the galaxy hosting BL Lacertae. At the 1978 conference devoted to BL Lac - type objects, it was suggested that the presence or absence of optical and/or UV emission lines is perhaps less relevant to the physical structure of blazars than their rapid variability, the existence of compact radio sources, and a large degree of polarization (cf. numerous articles in Wolfe 1978). The term “blazar,” dating back to that conference, includes both “lineless” BL Lac objects as well as “lined” quasars showing the same characteristics as BL Lac objects, plus emission lines. Independently, further observations of compact radio sources, particularly of their variability and of the detection of superluminal expansion, led to the suggestion that at least the matter responsible for the radio emission is moving at a relativistic speed at an angle close to the line of sight, perhaps in a jet-like structure (see, *e.g.*, Blandford & Rees 1978).

The most convincing evidence of similarity between the two sub-classes of blazars is the fact that both often show strong and variable GeV γ -ray emission (cf. von Montigny *et al.*1995). Of all classes of extragalactic sources, only blazars are strong GeV γ -ray emitters. In contrast, ordinary radio-quiet quasars and Seyfert galaxies, regardless of their optical, UV, and X-ray fluxes, are not detected above ~ 1 MeV. In general, blazars show two distinct peaks in their $E \times F(E)$ spectra, with one located in the infrared - through - X-ray band, and another located in the MeV to GeV (or even TeV) γ -rays (cf.

Von Montigny *et al.*1995). (In some cases, other, narrower peaks are present, but these are generally attributed to isotropic emission due to the host galaxy or the accretion disk.) The rapid variability observed in the γ -rays implies that the γ -ray source must be very compact. The simplest way to avoid an excessive opacity to $\gamma - \gamma$ pair production is to invoke relativistic boosting of γ -ray emission; most likely, the entire continuum emission in blazars is Doppler-boosted via a jet-like structure. BL Lacertae itself indeed shows GeV emission in the EGRET observations; in fact, the γ -ray flux ($E > 100$ MeV) increased from an upper limit of 30×10^{-8} photons $\text{cm}^{-2} \text{s}^{-1}$ in Oct. 1994 to a detection of $40 \pm 12 \times 10^{-8}$ photons $\text{cm}^{-2} \text{s}^{-1}$ in Jan. 1995 (cf. Catanese *et al.*1997).

X-ray surveys conducted over the last 20 or so years with satellites such as HEAO-A, Einstein Observatory, ROSAT, and *Asca*, revealed that BL Lac objects are generally strong X-ray emitters, with the X-ray spectrum generally well-described as a power law. (For a recent review, see, *e.g.*, Kubo *et al.*1998.) Those surveys revealed that the X-ray emission from BL Lac objects obeys a peculiar correlation: the ratio of the X-ray to optical fluxes was greater for objects where the ratio of the radio-to-optical fluxes was smaller (cf. Maraschi 1988). This correlation suggested that instead of dividing blazars by the presence/absence of emission lines, a better classification would rely on the overall spectrum. In this context, the BL Lac objects with the low energy peak located in the UV or X-rays – usually found via X-ray surveys – would be labeled as “High-energy peaked BL Lacs” or HBLs (cf. Giommi, Ansari, & Micol 1995), while those with the lower energy peak in the IR were labelled as “Low-energy peaked BL Lacs” or LBLs. The LBLs show broad-band spectra similar to blazars associated with lined, compact, flat radio-spectrum quasars (cf. Sambruna, Maraschi, & Urry 1986), which we will call here “quasar-hosted blazars,” or QHBs.

In this classification BL Lacertae is an LBL. Its spectrum peaks at $\sim 10^{14}$ Hz (cf.

Kawai *et al.*1991), and, historically, the optical spectrum was devoid of any emission lines. This changed within a few years before May 1995. A serendipitous observation at the Hale Observatories, intended for calibration purposes (Vermeulen *et al.*1995) revealed emission lines with equivalent $H\alpha$ width of $\sim 7 \text{ \AA}$ or more and FWHM of $\sim 4000 \text{ km s}^{-1}$. Corbett *et al.*(1996) confirmed the presence of the lines and inferred that the line flux increased four-fold. BL Lacertae, therefore, lost its defining characteristics. Interestingly enough, this happened around the epoch of the increase of the GeV flux.

Following reports that BL Lacertae entered an active, high state in June 1997 (Noble *et al.*1997), an impromptu monitoring campaign was organized. We observed it with the Rossi X-Ray Timing Explorer (RXTE) (Madejski, Jaffe, & Sikora 1997). The questions to be addressed were: what are the changes in the X-ray emission associated with the emergence of emission lines and the occurrence of the flare, and what constraints can the broad-band data impose on models of blazar jets? We report on X-ray observations (RXTE, as well as previous X-ray observations) in Sec. 2. In Sec. 3 and 4, we put the X-ray observations in the context of the broad-band spectrum and discuss the most plausible models for the radiative processes in the source, and in Sec. 5 we summarize our results.

2. OBSERVATIONS

Prior to the RXTE observation in June 1997 – which we describe in Sec. 2.3 – BL Lacertae was observed with the ROSAT PSPC and by *Asca*. We extracted these data from the HEASARC archives, and found that these show softer continuum and lower flux than the RXTE data. In addition, the well-exposed *Asca* data are very helpful in determining the low energy (photoelectric) absorption, which is probably not related to the source, and is assumed to be non-variable.

2.1. Asca Observations and Spectral Fitting

Asca observed BL Lacertae on 1995 November 22 for approximately 30 ks. The *Asca* data were screened using the `ftool ascascreen` and the standard screening criteria. The pulse-height data for the source were extracted using spatial regions with a diameter of 3' (for SISs) and 4' (for GISs) centered on the nominal position of BL Lacertae, while background was extracted from source-free regions of comparable size away from the source. The PHA data were subsequently rebinned to provide at least 20 counts per spectral bin. For the SIS data, we used the response matrix as appropriate for the observation epoch, generated via the `ftool sisrmg` v. 1.1; for the GIS data, we used the nominal (v. 4.0) response matrices. For both instruments, we used the telescope effective areas via the `ftool ascaarf` v. 2.72. The details of the observation (including the net counting rates) are given in Table 1.

We fitted the full-band PHA data using a simple power law absorbed at the low energies by neutral gas with Solar composition and cross-sections as given by Morrison & McCammon (1983); the results of the fits are given in Table 1. Using the data for all four *Asca* detectors over their full bandpass (0.6 – 10 keV), we get the following best fit (yielding χ^2 of 737 for 778 PHA channels): energy power law index $\alpha = 0.94 \pm 0.04$, and equivalent hydrogen column density of absorbing gas $N_{\text{H,X-ray}} = 2.7 \pm 0.2 \times 10^{21} \text{ cm}^{-2}$ (all errors are 90% confidence regions, meaning that they are determined from the values of fitted parameters at $\chi_{\text{min}}^2 + 2.7$).

While this fit is statistically acceptable, the value of the absorbing column in this simple absorbed power law model may be inconsistent with the Galactic value. Since BL Lacertae is located relatively close to the Galactic plane, it is necessary to consider the possible contribution from the Galactic molecular gas in addition to that associated with the usual 21 cm atomic hydrogen measurement. In the case of BL Lacertae, this was detected in

emission in ^{12}CO (Kazes & Crovisier 1981; Bania, Marscher, & Barvainis 1991) and in ^{13}CO (Crovisier, Kazes, & Brillet 1984), as well as in absorption in ^{12}CO (Marscher, Bania, & Wang 1991). The absorbing column consists therefore of two components: that associated with neutral hydrogen, inferred from the 21 cm measurements of Dickey *et al.*(1983) of $N_{\text{H},21\text{cm}}$ of $1.8 \times 10^{21} \text{ cm}^{-2}$, and the molecular component. Bania *et al.*(1991) measure an integrated CO emission W_{CO} of 4.6 K km s^{-1} , adopt the ratio $N_{\text{H},\text{mol}} / W_{\text{CO}}$ of $6 \times 10^{20} \text{ K}^{-1} \text{ km}^{-1} \text{ s cm}^{-2}$, and infer that the column of the molecular component corresponds to $N_{\text{H},\text{mol}}$ of $\sim 2.8 \times 10^{21} \text{ cm}^{-2}$, yielding the total column $N_{\text{H,tot}}$ of $\sim 4.6 \times 10^{21} \text{ cm}^{-2}$, significantly larger than $N_{\text{H},\text{X-ray}}$.

There are two possible reasons for this discrepancy. Regarding the CO measurements, the conversion of W_{CO} to $N_{\text{H},\text{mol}}$ may be unreliable (and direction-dependent); de Vries, Heithausen, & Thaddeus (1987) suggest that towards Ursa Major, the conversion of $N_{\text{H},\text{mol}} / W_{\text{CO}}$ of $1 \pm 0.6 \times 10^{20} \text{ K}^{-1} \text{ km}^{-1} \text{ s cm}^{-2}$ may be more appropriate. When applied to the case of BL Lacertae, this would yield $N_{\text{H},\text{mol}}$ of $\sim 0.5 \times 10^{21} \text{ cm}^{-2}$, and $N_{\text{H,tot}}$ of $\sim 2.3 \times 10^{21} \text{ cm}^{-2}$, which is now less than $N_{\text{H},\text{X-ray}}$. If the value of $N_{\text{H},21\text{cm}}$ is indeed accurate, one could obtain an agreement between $N_{\text{H},\text{X-ray}}$ and $N_{\text{H,tot}}$ using the conversion $N_{\text{H},\text{mol}} / W_{\text{CO}}$ of $\sim 2 \times 10^{20} \text{ K}^{-1} \text{ km}^{-1} \text{ s cm}^{-2}$, which is probably acceptable.

Alternatively, if the $N_{\text{H,tot}}$ of $\sim 4.6 \times 10^{21}$ derived by Bania *et al.*(1991) is indeed correct, this would imply that our simple power law model for the X-ray spectrum emitted by BL Lacertae is incorrect. This would then require that the intrinsic spectrum hardens towards higher energies. Such a gradually hardening spectrum is entirely possible, given the fact that the 1997 RXTE observation – with the bandpass extending beyond *Asca*'s – implies an even harder index than that in the simple power law model applied to the *Asca* data. As an alternative, we thus adopt a model consisting of a sum of two power laws, both absorbed by the fixed column suggested by Bania *et al.*(1991) of $4.6 \times 10^{21} \text{ cm}^{-2}$.

(We note here that a commonly used broken power law model for a description of such a hardening (concave) spectrum is unphysical, and we do not consider it here.) In this case, we obtain the “soft” power law index (dominating below ~ 1 keV) of 3.4 ± 0.7 and the “hard” index (dominating above ~ 1 keV) of $0.88^{+0.09}_{-0.14}$. This yields χ^2 of 736 for 778 PHA channels. We conclude that we cannot distinguish between the two models purely on the statistical basis. Nonetheless, the double power law model, if correct, may be attractive, suggesting that the *Asca* data reveal simultaneously the soft component – presumably the “tail” of the synchrotron emission – and the hard component, presumably the onset of the Compton component. However, we stress that this is *not* a unique representation of the *Asca* data, and more precise X-ray observations (with an instrument of better spectral resolution) are required to precisely measure the absorbing column via the measurement of the individual edges. In any case, the observed 2 – 10 keV flux of BL Lacertae during the 1995 November observation for either of the above models is $\sim 9 \times 10^{-12}$ erg cm $^{-2}$ s $^{-1}$, with a 10% nominal error. In the 0.5 – 2 keV band (useful for a comparison with the ROSAT data), it is $\sim 3.6 \times 10^{-12}$ erg cm $^{-2}$ s $^{-1}$, again with a 10% nominal error.

2.2. ROSAT PSPC Observations and Spectral Fitting

ROSAT observed BL Lacertae with the PSPC starting on December 22, 1992, in 2 short pointings about two days apart. The data were reduced using standard ROSAT PSPC procedures via the `ftool xselect` v. 1.4. The source PHA file was extracted from the event data using a circular extraction region of $3'$ in diameter, while the background was extracted from an annular region with the inner and outer diameters of $10'$ and $20'$, respectively. The data were fitted using the detector response matrix `pspcb_gain2_256.rmf` and telescope effective area file prepared using the `ftool pcarf` v. 2.1.1. The resulting counting rate was 0.16 ± 0.01 count s $^{-1}$ with no measurable variability apparent in the data.

A 2 ks observation of a relatively faint source with strong absorption such as BL Lacertae with an instrument with a relatively soft X-ray response such as the ROSAT PSPC yields data with only moderate statistical quality. Nonetheless, an interesting conclusion can be drawn by comparing these data against the *Asca* and the 21 cm / ^{12}CO data sets. An absorbed power law model of the form as above yields an acceptable fit (χ^2 is 30.4 for 40 PHA bins) with $\alpha = 4.1(-1.6, +2.4)$ and $N_H = 7 \pm 3 \times 10^{21} \text{ cm}^{-2}$; however, this best-fit value of the absorbing column is significantly higher than that inferred from the 21 cm / ^{12}CO or the *Asca* data. The most likely explanation is that the underlying continuum is more complex, curving downward. Independently of the severe conflict with the absorption measured by other instruments, such a steep power law cannot extend to lower energies indefinitely, and thus it must have a convex shape. Instead, such a shape may be approximated as a broken power law (which can be a physically realistic approximation of a spectrum; see, *e.g.*, the comment after Eq. 20), or an exponentially cutoff power law. Again, the quality of the data is modest, but to shed some light on the possible shape of the X-ray spectrum of BL Lacertae above ~ 1 keV in a very low state, we assumed that the absorbing column is indeed $2.7 \times 10^{21} \text{ cm}^{-2}$ and that the index below the break is the same as observed in *Asca*, $\alpha_{lo} = 0.9$. With this, we infer that for a broken power law model, the break energy E_b is $1.0 < E_b < 1.6$ keV, and the index above the break is $\alpha_{hi} > 2.2$ (χ^2 is 29.3). For an exponentially cutoff power law model with an underlying index $\alpha = 0.9$, we infer the e-folding energy E_c to be $1.0 < E_c < 2.3$ keV, with χ^2 of 34.8. Therefore a broken power law yields a better fit. The fits are summarized in Table 1; regardless of the model, the 0.5 – 2 keV flux is $\sim 1.5 \times 10^{-12} \text{ erg cm}^{-2} \text{ s}^{-1}$, with a nominal 10% error; this is roughly a half of the *Asca* flux in the same bandpass. In summary, when BL Lacertae was relatively faint, its intrinsic spectrum showed convex curvature and is well described by a phenomenological model of a broken power law.

2.3. RXTE Observations and Spectral Fitting

RXTE observations consisted of seven pointings over six days listed in Table 2; each pointing covered one or two orbits, interrupted only by the Earth occultations. These observations were scheduled during low-background orbits, i.e. those relatively free of passages through the South Atlantic Anomaly (SAA). The PCA instrument (Jahoda *et al.*1996) consists of 5 individual passively collimated, co-aligned, gas-filled proportional counter X-ray detectors, sensitive over the bandpass of 2 – 60 keV, each having an open area of $\sim 1300 \text{ cm}^{-2}$. The field of view of the instrument has roughly a triangular response, with FWHM of $\sim 1^\circ$. The HEXTE instrument (Rothschild *et al.*1998) consists of two detector clusters, each having four NaI / CsI scintillation counters, sensitive over the bandpass of 15 – 250 keV, with the total effective area of $\sim 1600 \text{ cm}^2$, and a field of view also of $\sim 1^\circ \times 1^\circ$.

For the PCA data, only three or four of the five detectors were operating. For maximum consistency among all observations, we used only the three detectors (known as PCU 0, 1, and 2) which were turned on for all the observations. The selection criteria were: the elevation angle over the Earth limb greater than 10° , and pointing direction less than 0.02° away from the nominal position of the source at $\text{RA}(2000) = 22^{\text{h}}02^{\text{m}}43^{\text{s}}.2$, $\text{Dec}(2000) = 42^\circ 16' 40''$.

2.3.1. PCA data

For a source as faint as BL Lacertae, more than half of the counts collected in the PCA are due to unrejected instrumental and cosmic X-ray background. To maximize the signal-to-noise ratio, we used only the top layer PCA data from the “Standard 2” mode.

The PCA background, instrumental plus cosmic, has been modeled from observations of blank (i.e. not near known X-ray sources) high latitude ($|b| > 30^\circ$) sky. The raw counting

rate varies with satellite latitude (i.e. with a period about half of the 96 minute orbital period) and with activation induced by the South Atlantic Anomaly (SAA). At least 3 time constants are present in the unrejected background (~ 20 minutes, ~ 4 hours, and ~ 4 days). The latitude variation is primarily due to the instantaneous particle environment while the activation is primarily due to the recent history of passages through the SAA. The background is parameterized by the so-called "L7" rate, which is derived from the two-fold coincidence Lower Level Discriminator (LLD) event rates present in the Standard 2 data (Jahoda *et al.*1996). In particular, "L7" consists of the instantaneous sum of signals derived from coincident "events" on anodes L1+R1, L2+R2, L1+L2, R1+R2, R3+L3, R2+R3, L2+L3 (Zhang *et al.*1993.) This rate tracks the particle-induced background as well as the short and long time constants. To this model, a time dependent term is added. The rate measured by the HEXTE particle monitor (the only detector onboard RXTE which operates during the SAA passages) is integrated through each SAA pass, and a term proportional to the sum of recent SAA rates $\times e^{-(t-t_{saa}/\tau)}$ is included. The spectral shape of this activation term is assumed to be constant, and the amplitude is determined by comparison of the observed total background in orbits just following SAA passages with the observed background in orbits far from SAA passages. The distribution of residuals to a background-subtracted count rate from a single blank sky region suggests a residual 1σ systematic error of $0.15 \text{ count s}^{-1}$ (3 PCUs, 2 - 10 keV) (see Jahoda *et al.*1999, in preparation). The resulting background-subtracted count rates for the 7 observations are shown in Table 2 and Fig. 1. Visual inspection indicates that the source varies significantly, and that the variability is undersampled; we can only state that the variability time scale is a day or less.

Since the data for the background estimation were collected from blank sky observations, the average Cosmic X-ray Background (CXB) is included in the background estimate, by construction. The contribution of the CXB flux to the total observed flux

in the PCA data can be scaled from the measurement given by Marshall *et al.*(1980) of $3.2 \text{ keV cm}^{-2} \text{ s}^{-1} \text{ sr}^{-1} \text{ keV}^{-1}$ at 10 keV, with a spectral shape well-approximated as a thermal bremsstrahlung with $kT = 40 \text{ keV}$. Since the solid angle of the PCA collimator is $\sim 3.2 \times 10^{-4} \text{ sr}$ (Jahoda *et al.*1996), the 2 - 10 keV flux is $1.7 \times 10^{-11} \text{ erg cm}^{-2} \text{ s}^{-1}$.

While it is possible to estimate the contribution of the *mean* CXB flux, the CXB is not uniform from all directions in the sky. The fluctuations in the CXB on the solid angle scale of the PCA collimator can be estimated by scaling the HEAO-1 A2 fluctuations by the ratio of square root of the solid angles of A2 and PCA detectors (Shafer 1983; Mushotzky & Jahoda 1992, Fig. 1, with the correction that the mean counting rate should be 3.5 count s^{-1} , and not 5.6 count s^{-1} as stated in the caption). The 1σ CXB fluctuation is about 10% of the CXB contribution, or $\sim 0.2 \text{ count s}^{-1}$ per PCA detector (2 – 10 keV). While the variability can be reliably measured at much smaller levels, this represents a limiting uncertainty in the determination of the absolute flux for observations using the PCA alone.

2.3.2. *HEXTE data*

The HEXTE background is continuously measured, as each cluster alternately rocks to one of two off-source pointings (on alternate 16 second intervals for this observation). This gives an effectively simultaneous background measurement at four positions around the source. This background is dominated by internal activation (Gruber *et al.*1996). A significant instrument deadtime (15 – 40%), however, introduces some uncertainty in the absolute flux level. This deadtime is largely particle-induced and is therefore significant even for faint sources. A deadtime correction factor is calculated from the charged particle rates to bring the exposure to within a few percent of its actual value (based on 16 s timescale observations of the Crab). The resulting residuals for the background estimation using this procedure are 1% of background or less (Rothschild *et al.*1998). However, while

BL Lacertae was detected with HEXTE at ~ 0.5 net count s^{-1} , each data segment had too low a signal-to-noise ratio to measure the spectrum, and we could only do so for the summed data (cf. Table 2).

2.3.3. Spectral fitting of the RXTE data

We fit the PHA spectrum from each observation to a model including a simple power law which is photoelectrically absorbed at low energies by neutral gas with Solar abundances and with cross-sections given by Morrison & McCammon (1983) with a fixed column density of $2.7 \times 10^{21} \text{ cm}^{-2}$ as determined from the *Asca* observations. (We note that adopting a column of $4.6 \times 10^{21} \text{ cm}^{-2}$ does not change our conclusions significantly.) In our fits, we used the instrumental response matrix generated via `ftool pcarmf v. 3.5`, which corrects for the slight PCA gain drift ($\sim 1\%$ over 2 years) and energy – to – channel conversion table `pca_e2c_e03v04.fits`, as appropriate for the observation epoch of BL Lacertae. The results in Table 2 indicate that the data for each pointing are well-described by the absorbed power law model, but we do observe spectral variability from one pointing to another, with the energy power law index α varying from 0.42 ± 0.08 to 0.80 ± 0.06 , with no clear correlation of the index with the flux level. To determine the average spectral shape to the highest possible energies (where additional information is gained from the HEXTE data), we also co-added all data.

For simultaneous analysis of PCA and HEXTE data, there is some uncertainty in the relative normalization which must be taken into account. This difference is not determined uniquely as yet, but in general, the PCA agrees more closely with previous data (namely OSSE and *Ginga*) and is therefore taken as the baseline against which the HEXTE data are normalized. This factor is generally ~ 0.7 for the fits using the effective areas released in `ftools v. 4.1`. The addition of the HEXTE data does not change the resulting spectral

fit parameters, but implies that the hard X-ray spectrum observed in PCA extends to higher energies (~ 70 keV); the summed PCA and HEXTE spectra are plotted in Fig. 2. The best-fit spectral model gives a mean 2 – 10 keV flux of $2.6 \pm 0.3 \times 10^{-11}$ erg cm $^{-2}$ s $^{-1}$. This value has an additional associated uncertainty of $\sim 0.2 \times 10^{-11}$ erg cm $^{-2}$ s $^{-1}$ from the fluctuations of the CXB.

3. DISCUSSION

The RXTE observations of BL Lacertae conducted in July 1997 show that the source was bright and variable in the X-ray band, with the X-ray spectrum significantly harder than observed during the periods of lower brightness and activity; the mean 2 – 10 keV flux was 2.6×10^{-11} erg cm $^{-2}$ s $^{-1}$, about 3 times greater than that observed by *Asca* in November 1995. A direct comparison with the ROSAT PSPC observation in December 1992 is not possible, but the 0.5 – 2 keV flux in 1992 was about a half of that in Nov. 1995, so the mean July 1997 flux must have been at least 6 times greater than in December 1992. BL Lacertae was also observed by *Ginga* in 1988 (Kawai *et al.*1991). The June 15 1988 observation implies a 2 – 10 keV flux of 7.6×10^{-12} erg cm $^{-2}$ s $^{-1}$ with α of 0.71 ± 0.07 , while for July 17 1988 observation, the 2 – 10 keV flux was 5.5×10^{-12} erg cm $^{-2}$ s $^{-1}$ with α of 1.16 ± 0.24 . In general, the X-ray spectrum of BL Lacertae appears to be harder when the source is brighter. This is illustrated in Fig. 3, where we plot the unfolded summed PCA spectrum together with the *Asca* GIS and ROSAT PSPC spectra.

The analysis of the *Asca* data by Kubo *et al.*(1998), as well as many papers published earlier (cf. Sambruna *et al.*1996; Worrall & Wilkes 1990), imply that HBL-type blazars generally have relatively soft X-ray ($\alpha > 1$) spectra, while QHBs show harder spectra, with $\alpha < 1$. The spectra of LBLs, the class of objects where BL Lacertae belongs, are intermediate. For BL Lacertae, the shape of the spectrum is related to the state of the

source. Interestingly, the X-ray spectral characteristics of BL Lacertae appear to be “HBL-like” when the emission lines are weak or absent, and “QHB-like” when the emission lines are strong; an intriguing possibility (although by no means certain, depending on the details of the Galactic absorption; cf. Section 2.1) is that during the intermediate state of the source, shortly after the emergence of the emission lines, the spectrum simultaneously consisted of both the LBL-like (hard) and HBL-like (soft) components, with comparable fluxes at ~ 1 keV.

The observations of blazars imply that the entire continuum (including both the low- and high-energy components mentioned in Sec. 1) arises in a relativistic jet. The polarization and the local power-law shape of the spectrum of the low energy component suggest that the process responsible for emission in this spectral region is synchrotron radiation by highly relativistic electrons, accelerated by an as yet unknown mechanism. For the high energy peak, the best current model is Compton-upscattering of soft photons by the same electrons that produce synchrotron radiation via interaction with magnetic field. The origin of those soft photons is under debate: they can be either synchrotron photons internal to the jet, as in synchrotron self-Compton models (cf. Blandford & Königl 1979; Königl 1981; Ghisellini & Maraschi 1989), or they can be external to the jet, either from the accretion disk (Dermer, Schlickeiser, & Mastichiadis 1992), or else from broad emission line clouds and/or intercloud material (Sikora, Begelman, & Rees 1994). Perhaps the best current picture has the former mechanism dominating the γ -ray emission in HBL-type blazars, which usually do not show broad emission lines (but see, *e.g.*, Padovani *et al.*1998), while the latter dominates in QHBs, blazars associated with quasars (cf. Madejski *et al.*1997). In this context, the soft X-ray spectra of HBLs are the “tails” of the synchrotron component (and thus produced by the most energetic electrons), while the hard spectra of QHBs are emitted via the Compton process by the lower energy electrons.

The overall broad-band spectrum of BL Lacertae, including the July 1997 data, is plotted in Fig. 4. The two peaks generally present in blazar spectra are apparent in the plot. However, the fact that the γ -ray spectrum is hard – with a spectral index which is lower (harder) than the two-point spectral index between the hard X-rays and the beginning of the EGRET spectrum – and that it lies below the extrapolation of the X-ray power-law spectrum, suggests that the total high energy spectrum consists of two separate components. Below, we follow the suggestion presented by us at the November 1997 HEAD meeting that the high energy spectrum of this source as measured in July 1997 actually consists of two components, one radiated via the synchrotron self-Compton process, dominating in the X-ray band, and another radiated via external-radiation-Compton, dominating in the GeV γ -ray band, and in the context of such a scenario, we estimate the physical parameters of the radiating plasma.

4. THEORETICAL MODELS

In our study of the radiative processes operating in the jet of BL Lacertae, we use the instantaneous spectrum averaged over the available July 1997 data that are simultaneous with the EGRET observation (Fig. 4). The optical data (Bloom *et al.*1997) show that the July 1997 high state of BL Lacertae is a superposition of many flares (and probably the same is true for other spectral bands). We thus interpret these flares as a result of the formation of relativistic shocks, which, within a given distance range in a jet, effectively accelerate relativistic particles. We assume that the transverse size of these shocks is

$$a \simeq c\Delta t\Gamma, \tag{1}$$

where Δt is the observed time scale of the flare and Γ is the bulk Lorentz factor of the radiating matter.

We investigate two models, the SSC (synchrotron-self-Compton) where the GeV radiation results from Comptonization of the intrinsic synchrotron radiation, and the ERC (external-radiation-Compton) where the GeV radiation is produced by Comptonization of the broad emission line light. The models are specified by adopting the following parameters describing activity of BL Lac in July 1997:

- location of the peak of the low-energy (synchrotron) component - $h\nu_S \sim 1\text{eV}$;
- location of the peak of the high-energy (Compton) component - $h\nu_C \geq 10\text{GeV}$;
- synchrotron luminosity - $L_S \sim 2 \times 10^{45} \text{ erg s}^{-1}$;
- Compton luminosity - $L_C \sim 8 \times 10^{45} \text{ erg s}^{-1}$;
- time scale of a flare - $\Delta t \sim 8 \text{ hrs}$;
- typical energies corresponding to broad emission line frequencies - $h\nu_L \sim 10 \text{ eV}$;
- energy spectral index in the X-ray band - $\alpha_X \sim 0.5$.

To determine the parameters of the ERC model, we also need to know the luminosity of the external radiation. We derive it by using the measurements of the H_α line in June 1995 (Corbett *et al.*1996) and by assuming that the line intensity ratios in BL Lacertae are the same as those in quasars. Using the “line-bolometric” correction (Celotti, Padovani & Ghisellini 1997), we find $L_{BEL} \sim 4 \times 10^{42} \text{ erg s}^{-1}$ and adopt it for the July 1997 flare.

4.1. Synchrotron Self-Compton

In the SSC model, $\nu_C \equiv \nu_{SSC}$, and we have

$$h\nu_S \simeq \gamma'_m{}^2 (B'/B_{cr}) \Gamma m_e c^2 \quad (2)$$

and

$$h\nu_C \simeq h\nu_S \gamma'_m{}^2, \quad (3)$$

where B' is the intensity of the magnetic field, $B_{cr} \equiv 2\pi m_e^2 c^3 / h e \simeq 4.4 \times 10^{13}$ Gauss, and γ'_m is the Lorentz factor at which the energy distribution of electrons has a high energy break/cutoff. All primed quantities are measured in the comoving frame of the flow in the active region.

Assuming that observer is located at an angle $\theta_{obs} \sim 1/\Gamma$ from the jet axis and noting that $L_S \sim \Gamma^4 L'_S$, we find that the ratio of the SSC peak luminosity to the synchrotron luminosity is given by (Sikora *et al.*1994; Ghisellini, Maraschi, & Dondi 1996)

$$\frac{L_C}{L_S} = \frac{u'_S}{u'_B} \simeq \frac{L'_S}{4\pi a^2 c} \frac{8\pi}{B'^2} \simeq \frac{2L_S}{c^3 \Delta t^2 \Gamma^6 B'^2}. \quad (4)$$

Now, combining eqs. (1) – (4), and substituting the values adopted by us for BL Lacertae, we find

$$\Gamma \simeq \left(\frac{L'_S}{L_C} \frac{\nu_C^2}{\nu_S^4} \frac{1}{\Delta t^2} \frac{2m_e^2 c}{h^2 B_{cr}} \right)^{1/4} \sim 100, \quad (5)$$

$$B' = \frac{1}{\Gamma} \frac{\nu_S^2}{\nu_C} \frac{h B_{cr}}{m_e c^2} \sim 10^{-4} \text{ Gauss}, \quad (6)$$

and

$$\gamma'_m = \sqrt{\frac{\nu_C}{\nu_S}} \sim 10^5. \quad (7)$$

For such model parameters, the low energy spectral break predicted to arise due to synchrotron self-absorption should be located at a frequency ν_a given by

$$\nu_a \simeq 1.7 \times 10^2 B'^{1/7} (L_\nu \nu)_{\nu=\nu_a}^{2/7} \Delta t^{-4/7} \Gamma^{-5/7} \sim 1.3 \times 10^{10} \text{ Hz}, \quad (8)$$

This is lower than the observed value by at least a factor of 10 – 30 (see, *e.g.*, Bregman *et al.*1990). It should be emphasized here that because no signature of the high-energy break is observed up to the highest energies covered by EGRET, the value $h\nu_C = 10$ GeV used here is actually the lowest plausible value of the location of the high energy break, and that for a larger $h\nu_C$, the output model parameters become even more extreme.

4.2. External Radiation-Compton

The discovery of broad emission lines in BL Lacertae (Vermeulen *et al.*1995; Corbett *et al.*1996) indicates that in this object, just as in the case of quasars, the subparsec jet is embedded in a diffuse radiation field. The energy density of this field as measured in the comoving frame of the blob is thus amplified by a factor $\sim \Gamma^2$. The rate of the electron energy losses due to Comptonization of this radiation can then be approximated by (Sikora *et al.*1994)

$$\frac{d\gamma'}{dt'} \simeq \frac{c\sigma_T u'_{ext}}{m_e c^2} \gamma'^2, \quad (9)$$

where

$$u'_{ext} \sim \frac{L_{BEL}\Gamma^2}{4\pi r^2 c}, \quad (10)$$

and r is the distance of an active region from the central object (black hole). For an opening half-angle of a jet $\theta_j \sim a/r \sim 1/\Gamma$, and for an observer located within or close to the jet cone, the ratio of the ERC peak luminosity to the synchrotron peak luminosity is given by (Sikora 1997):

$$\frac{L_C}{L_S} \simeq \frac{u'_{ext}}{u'_B} \simeq \frac{2L_{BEL}\Gamma^2}{r^2 c B'^2} \simeq \frac{2L_{BEL}}{c^3 \Delta t^2 B'^2 \Gamma^2}, \quad (11)$$

where now

$$\nu_C \simeq (\gamma'_m \Gamma)^2 \nu_L. \quad (12)$$

Combining equations (2), (11), and (12), we obtain

$$\Gamma \simeq \left(\frac{2L_S L_{BEL}}{L_C} \right)^{1/4} \left(\frac{\nu_C}{\nu_L \nu_S} \frac{1}{\Delta t} \frac{m_e c^{1/2}}{h B_{cr}} \right)^{1/2} \sim 8, \quad (13)$$

$$B' = \Gamma \frac{\nu_S \nu_L \Gamma}{\nu_C} \frac{h B_{cr}}{m_e c^2} \sim 1 \text{ Gauss}, \quad (14)$$

and

$$\gamma'_m \simeq \frac{1}{\Gamma} \left(\frac{\nu_C}{\nu_L} \right)^{1/2} \sim 4 \times 10^3. \quad (15)$$

For these parameters, $\nu_a \simeq 4 \times 10^{11}$ Hz, which is consistent with the observations (Bregman *et al.*1990). In addition, the relatively low value of Γ is consistent with both the superluminal expansion data (cf. Mutel & Phillips 1982) and with the limits derived from the considerations of the compactness of the source as inferred from the variability data via opacity to pair production.

4.3. ERC Radiation plus SSC Radiation

Provided that both ERC and SSC spectral components are produced in the Thomson regime and that the observer is located within or near the jet cone, the ratio of the peak luminosities of these two components can be approximated by the formula

$$\frac{L_{SSC}}{L_{ERC}} \simeq \frac{u'_S}{u'_{ext}} \simeq \frac{1}{\Gamma^4} \frac{L_S}{L_{BEL}}, \quad (16)$$

Assuming that the γ -rays are produced by the ERC mechanism, we use in eq. (12) $\Gamma \simeq 8$ and $\gamma'_m \simeq 4 \times 10^3$ (see §3.2) and obtain a luminosity of the SSC radiation of $L_{SSC} \simeq 0.2 L_{ERC} \simeq 0.6 \times 10^{46}$ erg s⁻¹ and a location of its peak at $h\nu_{SSC} \simeq \gamma'_m{}^2 \nu_S \simeq 15$ MeV. The two spectral components, the SSC and the ERC, overlap for $\Gamma^2 \nu_L < \nu < \nu_{SSC}$. In this range,

$$\frac{L_{SSC\nu}}{L_{ERC\nu}} \simeq \left(\frac{\gamma'_{(SSC)}}{\gamma'_{(ERC)}} \right)^{2(1-\alpha_X)} \frac{u'_S}{u'_{ext}} \simeq \left(\frac{h\nu_L}{m_e c^2} \frac{B_{cr}}{B'} \frac{\Gamma}{\gamma'_m{}^2} \right)^{1-\alpha_X} \frac{L_S}{L_{BEL}} \frac{1}{\Gamma^4} \sim 10, \quad (17)$$

where $\gamma'_{(ERC)} \simeq \sqrt{\nu/\nu_L}/\Gamma$ and $\gamma'_{(SSC)} \simeq \sqrt{\nu/\nu_S}$ are the energies of the electrons contributing to the radiation at a frequency ν via ERC and SSC process, respectively.

This combined synchrotron + SSC + ERC model predicts that all three spectral components should have a break due to adiabatic losses of electrons below a certain energy. Since radiative energy losses are dominated by the ERC process, the corresponding break energy of the electron distribution, γ'_b , can be found from equating the time scale of the

ERC energy losses, $t_{ERC} \simeq \Gamma\gamma'/(d\gamma'/dt')_{ERC}$, to the time scale of the propagation of the perturbed flow pattern, $\Delta t\Gamma^2$. Using eqs. (9) and (10), we obtain

$$\gamma'_b \simeq \frac{4\pi m_e c^4}{\sigma_T} \frac{\Delta t\Gamma}{L_{BEL}} \sim 10^3. \quad (18)$$

The presence of this break in the electron distribution should result in a change of slope of $\Delta\alpha \simeq 0.5$ (Sikora *et al.*1994) in all three spectral components. Note that during a flare, the spectrum most likely would vary in time as a result of the effective change of the spectral slope due to the change of the location of this break. In our case, we model the time averaged spectrum; in particular, the adiabatic losses of electrons with $\gamma' < \gamma'_b$ result in the change of the spectral slope at $\nu(\gamma_b)$, and the data indeed show $\Delta\alpha \simeq 0.5$. In the synchrotron component the break occurs around 0.2 eV, while in the SSC component it is around 0.75 MeV, and in the ERC spectral component around 0.5 GeV. As calculated from the electron kinetic equation, this break is very smooth, and since γ'_b is very close to the maximum electron energy, the “adiabatic” breaks should join smoothly with the intrinsic high energy breaks. This is illustrated in Fig. 4, where the data for the July 1997 flare are fitted with our ERC+SSC model.

As one can see from Fig. 4, the SSC component, calculated self-consistently within the framework of the ERC model, fits the X-ray data reasonably well. We note that such a three-component spectral structure was also inferred by Kubo *et al.*(1998) for other QHB blazars. Our result is that the high energy (> 3 keV) spectrum of BL Lacertae is more similar to blazars associated with quasars (QHBs) than to HBLs, further strengthening the inference that LBLs are weak-lined quasars, and that HBLs form a somewhat distinct subclass of BL Lac type objects. We also note that in the context of this model, the overall spectrum of BL Lacertae (and, by similarity, that of most other LBL-type blazars) is *not* expected to extend to the TeV energies. This is because the distribution of the relativistic electrons does not extend to sufficiently high energies to produce TeV γ -rays,

while the second-order Comptonization is inefficient because of the drop in the Compton cross-section due to the Klein-Nishina limit. This is in contrast to HBLs, where electron energy distributions extend to a range that can be $10^2 - 10^3$ times greater (Kubo *et al.*1998) than that derived above.

5. SUMMARY

We summarize as follows:

- (1) The RXTE observations of BL Lacertae in July 1997, during the flare observed in the ground-based optical and γ -ray EGRET data, imply that the source was bright in the X-ray band. The X-ray spectrum was relatively hard, exhibiting both flux and spectral variability with a mean energy power law index α of 0.59. The source showed a peak in its X-ray flux nearly coincident with the peak of the GeV γ -ray flux.
- (2) A comparison of the RXTE data to the archival *Asca* and ROSAT PSPC data implies that the spectrum of BL Lacertae is generally harder when the source is brighter. The *Asca* data possibly show an additional soft component above the extrapolation of the hard power law to lower energies (but the presence of this soft component is uncertain and subject to the details of the Galactic absorption). This general spectral behavior appears to be associated with an emergence of broad emission lines in BL Lacertae first reported in 1995.
- (3) The broad-band spectrum of BL Lacertae appears more similar to a blazar associated with a quasar than to the more common HBL - type, “certified lineless” sub-class of blazars, implying an association of the presence of the broad emission lines with the high energy portion of the overall spectrum. This further supports the suggestion of Vermeulen *et al.*(1995) that BL Lacertae is no longer a BL Lac object; this seems to be true of the high energy portion of its spectrum as well.

(4) The broad-band spectrum of BL Lacertae cannot be readily fitted with either the synchrotron self-Compton (SSC) or the External Radiation Compton (ERC) model. However, a hybrid model, where the X-ray radiation arises via the SSC process and the GeV γ -ray radiation is produced via ERC, can fit the data well. From this model, we derive the bulk Lorentz factor of the jet $\Gamma \sim 8$, magnetic field $B \sim 1$ Gauss, and Lorentz factors γ'_m of the electrons radiating in all three components at the peak of their respective $\nu \times F(\nu)$ distributions to be $\sim 4 \times 10^3$.

We acknowledge the referee, Dr. Marscher, for his comments leading to significant improvements to this paper, and the support from NASA RXTE observing grants to GSFC via Universities Space Research Association (USRA), and Polish KBN grant 2P03D00415.

REFERENCES

- Bania, T., Marscher, A. P., & Barvainis, R. 1991, AJ, 101, 2147
- Blandford, R. D., & Königl, A. 1979, ApJ, 232, 34
- Blandford, R. D., & Rees, M. J. 1978, in Pittsburgh Conference on BL Lac Objects, ed. A. M. Wolfe (Pittsburgh University Press), p. 328
- Bloom, S. D., *et al.*1997, ApJ, 490, L145
- Bregman, J. N., *et al.*1990, ApJ, 352, 574
- Catanese, M., *et al.*1997, ApJ, 480, 562
- Celotti, A., Padovani, P., & Ghisellini, G. 1997, MNRAS, 286, 415
- Corbett, E. A., Robinson, A., Axon, D. J., Hough, J. H., Jeffries, R. D., Thurston, M. R., & Young, S. 1996, MNRAS, 281, 737
- Crovisier, J., Kazes, I., & Brillet, J. 1984, *å*, 138, 237
- Dermer, C. D., Schlickeiser, R., & Mastichiadis, A. 1992, *å*, 256, L27
- de Vries, H. W., Heithausen, A., & Thaddeus, P. 1987, ApJ, 319, 723
- Dickey, J. M., Kulkarni, S. R., van Gorkom, J. H., & Heiles, C. E. 1993, ApJS, 53, 591
- DuPuy, D., Schmitt, J., McClure, R., van den Bergh, S., & Racine, R. 1969, ApJ, 156, L135
- Ghisellini, G., & Maraschi, L. 1989, ApJ, 340, 181
- Ghisellini, G., Maraschi, L., & Dondi, L. 1996, A&AS, 120, C503
- Giommi, P., Ansari, S. G., & Micol, A. 1995, A&AS, 109, 267
- Grove, J. E. & Johnson, W. N. 1997, IAU Circular 6705
- Gruber, D., *et al.*1996, A&AS, 120, 641
- Hartman, R., *et al.*1997, IAU Circular 6703

- Hewitt, A. & Burbidge, G. 1993, ApJS, 87, 451
- Jahoda, K., Swank, J. H., Giles, A. B., Stark, M. J., Strohmayer, T., Zhang, W., & Morgan, E. H. 1996, in “EUV, X-ray, and Gamma-ray Instrumentation for Astronomy VII”, SPIE Proceedings, O. Siegmund & M. Gummin, eds, 2808, 59
- Kawai, N., *et al.* 1991, ApJ, 382, 508
- Kazes, I., & Crovisier, J. 1981, *Å*, 101, 401
- Königl, A. 1981, ApJ, 243, 700
- Kubo, H., Takahashi, T., Madejski, G., Tashiro, M., Makino, F., Inoue, S., & Takahara, F. 1998, ApJ, 504, 693
- Ma, F., & Barry, D. 1997, IAU Circular 6703
- Maesano, M., Massaro, E., & Nesci, R. 1997, IAU Circular 6700
- Madejski, G., Jaffe, T. & Sikora, M. 1997, IAU Circular 6705
- Madejski, G., *et al.* 1997, in “X-ray Imaging and Spectroscopy of Cosmic Hot Plasmas,” F. Makino & K. Mitsuda, eds. (Tokyo: Universal Academy Press), 229
- Maraschi, L., Maccacaro, T., & Ulrich, M.-H (eds) 1989, “BL Lac Objects” (Springer-Verlag: Berlin)
- Marshall, F. E., *et al.* 1980, ApJ, 235, 4
- Marscher, A. P., Bania, T. M., & Wang, Z. 1991, ApJ, 371, L77
- Miller, J. S., & Hawley S. A. 1977, ApJ, 212, L47
- Morrison, R., & McCammon, D. 1983, ApJ, 270, 119
- Mushotzky, R. F., & Jahoda, K. 1992, in “The X-ray Background,” X. Barcons & A. Fabian, eds. (Cambridge University Press), 80

- Mutel, R., & Phillips, R. 1982, in “Extragalactic Radio Sources,” Proc. IAU Symp. 97, D. Heeschen & C. M. Wade, eds. (Doerrecht: Riedel), 385
- Noble, J. C., *et al.* 1997, IAU Circular 6693
- Oke, J. B., Neugerbauer, G., & Becklin, E. E. 1969, ApJ, 156, L41
- Padovani, P., Perlman, E., Giommi, P., & Sambruna, R. 1998, BAAS, 30, 1413
- Rothschild, R. E., *et al.* 1998, ApJ, 496, 538
- Sambruna, R., Maraschi, L., & Urry, C. M. 1996, ApJ, 463, 444
- Schmitt, J. 1968, Nature, 218, 663
- Seaton, M. J. 1979, MNRAS, 187, 73p
- Shafer, R. 1983, PhD thesis, University of Maryland, College Park
- Sikora, M. 1997, in “Proceedings of the Fourth Compton Symposium” (AIP Conference Proceedings 410), eds C. D. Dermer, M.S . Strickman & J. D. Kurfess, 494
- Sikora, M., Begelman, M. C., & Rees, M. J. 1994, ApJ, 421, 153
- Strittmatter, P. A., Serkowski, K., Carswell, R. F., Stein, W. A., Merrill, K. M., & Burbidge, E. M. 1972, ApJ, 175, L7
- Vermeulen, R. C., Ogle, P. M., Tran, H. D., Browne, I. W. A., Cohen, M. H., Readhead, A. C. S., & Taylor, G. B. 1995, ApJ, 452, L5
- Véron-Cetty, M.-P. & Véron P. 1996, ESO Publication No. 17
- Von Montigny, C., *et al.* 1995, ApJ, 440, 525
- Wolfe, A. (ed.) 1978, Pittsburgh Conference on BL Lac Objects, (Pittsburgh University Press)
- Worrall, D., & Wilkes, B. 1990, ApJ, 360, 396

Zhang, W., Giles, A. B., Jahoda, K., Swank, J. H., & Morgan, E. M. 1993, in “EUV, X-ray, and Gamma-ray Instrumentation for Astronomy IV,” SPIE Proceedings, O. Siegmund ed., 2006, 324

FIGURE CAPTIONS

Fig. 1.— Light curve obtained from the PCA RXTE observations for BL Lacertae in July 1997 over the 3 – 20 keV bandpass. The observations are most likely undersampled, but the highest point in the PCA light curve roughly corresponding to the highest point in the EGRET light curve, apparent on 19 July 1997 (cf. Fig. 2 in Bloom *et al.*1997). The systematic background subtraction errors are ~ 0.3 count s^{-1} , while the unknown but constant offset due to the fluctuations of the Cosmic X-ray Background is ~ 0.6 count s^{-1} (1σ).

Fig. 2.— Combined July 1997 RXTE PCA and HEXTE data (top panel) and residuals (bottom panel) to a simple power law model for the spectrum of BL Lacertae.

Fig. 3.— Unfolded X-ray spectra for BL Lacertae obtained in December 1992 by ROSAT PSPC, November 1995 by *Asca*, and July 1997 by RXTE PCA. These data illustrate the point that the X-ray spectrum of BL Lacertae appears harder when the source is brighter.

Fig. 4.— Broad-band spectrum of BL Lacertae in July 1997. DATA FROM JULY 1997: crosses - optical data (Maesano, Massaro, & Nesci 1997; Ma & Barry 1997); solid line “bowtie” in the 2 – 10 keV band – RXTE average of the summed July 1997 data (this paper); solid line “bowtie” in the 50 – 300 keV band – OSSE time averaged data from the period 15 – 21 July (Grove & Johnson 1997); solid line “bowtie” in the $E > 100$ MeV range – time averaged EGRET data from the period 15 – 22 July (Hartman *et al.*1997; Bloom *et al.*1997). DATA FROM OTHER EPOCHS: dots – optical, infrared and radio data from various epochs (NED; Véron-Cetty & Véron 1996; Hewitt & Burbidge 1993); X-rays from *Ginga* (2 – 30 keV range from 15 June and 17 July 1988 [Kawai *et al.*1991]), EXOSAT (1 – 5.6 keV range from 8 June 1980 [Bregman *et al.*1980]), and from *Asca* (dotted line “bowtie” in the 2 – 10 keV range from 22 November 1995 [this paper]); γ -rays from EGRET (dotted line “bowtie” in the $E > 100$ MeV from January 1995 [Catanese *et al.*1997]). All optical data are dereddened under assumption $E(B - V) = 0.31$ (Bregman 1990) and using algorithm of Seaton (1979). The long-dashed lines show our theoretical model, which includes three components: the synchrotron component dominating in the radio - to - UV range, the synchrotron self-Compton component in the X-ray range, and the external radiation Compton component dominating in the MeV - GeV range.

XTE light curve of BL Lacertae in July 1997

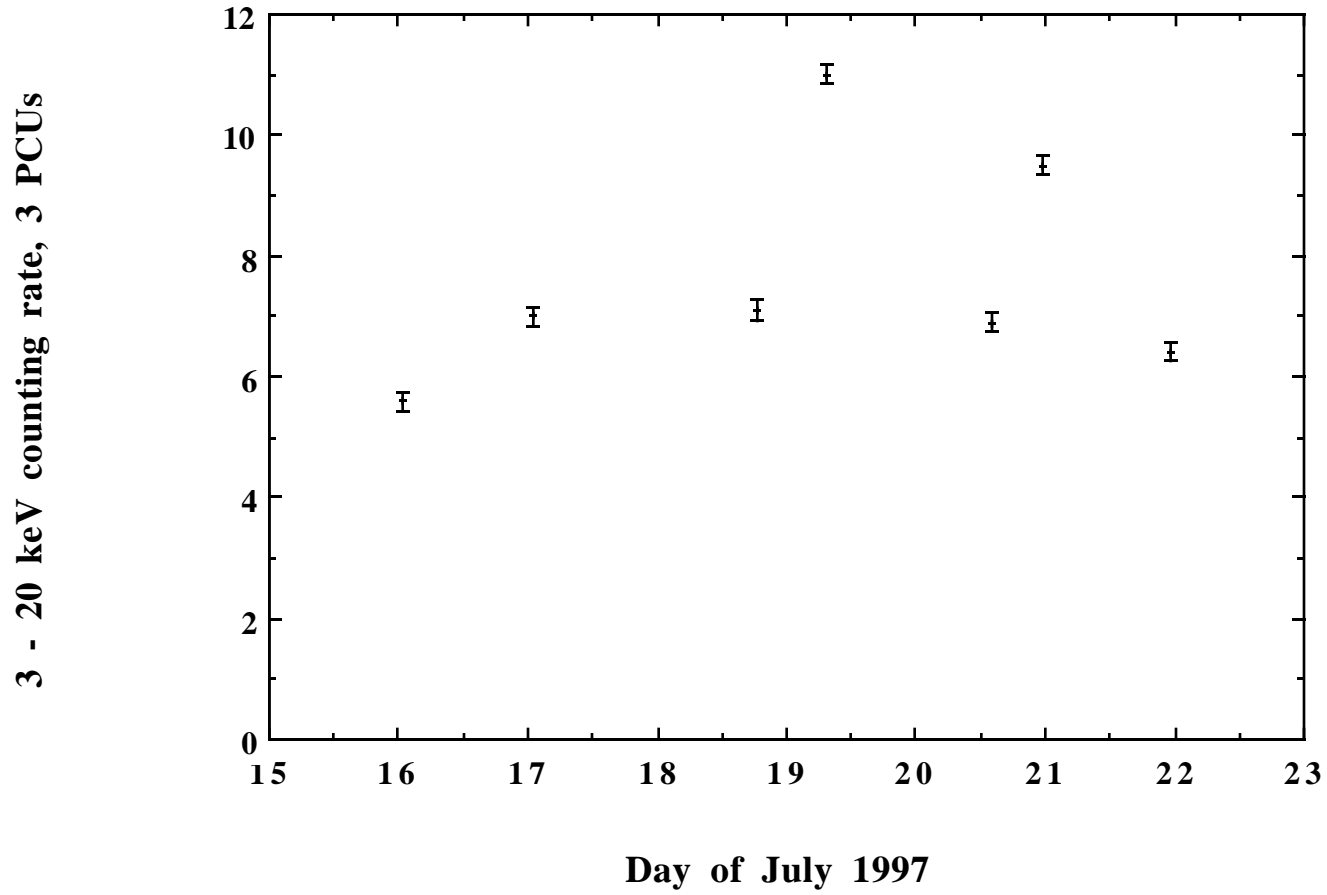


TABLE 1
ROSAT PSPC AND ASCA OBSERVATIONS OF BL LACERTAE

ROSAT PSPC					
Date (UT)	Observ. length (s)	Ct. rate & error	0.5 – 2 keV Flux		
12/22/92	2167	0.16 ± 0.01	0.15×10^{-11}		
Model	Fit parameters & error			χ^2	
Power law	$N_{\text{H}} = 7 \pm 3 \times 10^{21}$, $\alpha = 4.1_{-1.6}^{+2.4}$			30.4/40 PHA ch.	
Broken PL	$N_{\text{H}} = 2.7^F \times 10^{21}$, $\alpha_l = 0.9^F$, $1.0 < E_b < 1.6$ keV, $\alpha_h > 2.2$			29.3/40 PHA ch.	
Exp. cut PL	$N_{\text{H}} = 2.7^F \times 10^{21}$, $\alpha = 0.9^F$, $1.0 < E_c < 2.3$ keV			34.8/40 PHA ch.	
ASCA					
Date (UT)	Exposure (s) & Ct. rate / error (count s ⁻¹)				2 – 10 keV Flux
	SIS0	SIS1	GIS2	GIS3	
11/22/95	26017	26952	27047	27047	0.9×10^{-11}
	0.296 ± 0.004	0.233 ± 0.003	0.172 ± 0.003	0.220 ± 0.003	
Fit parameters & errors for combined GIS and SIS data:					
Absorbed power law model (free column), fitted over 0.6 – 10 keV to all data				χ^2	
$N_{\text{H}} = 2.7 \pm 0.2 \times 10^{21}$, $\alpha = 0.94 \pm 0.04$				737/778 PHA ch.	
Double power law model absorbed by a fixed column, fitted over 0.6 – 10 keV to all data				χ^2	
$N_{\text{H}} = 4.6^F \times 10^{21}$, $\alpha_{\text{lo}} = 3.4 \pm 0.7$, $\alpha_{\text{hi}} = 0.88_{-0.14}^{+0.09}$				736/778 PHA ch.	

NOTE.— ROSAT data are fitted over the 0.2 – 2 keV band. Asca count rates are over the 0.6 – 10 keV band. Absorbing column density is in units of H atoms per cm². Flux is in units of erg cm⁻² s⁻¹. The superscript ^F means that the fit parameter was fixed at the given value.

RXTE PCA and HEXTE July 1997 data for BL Lacertae

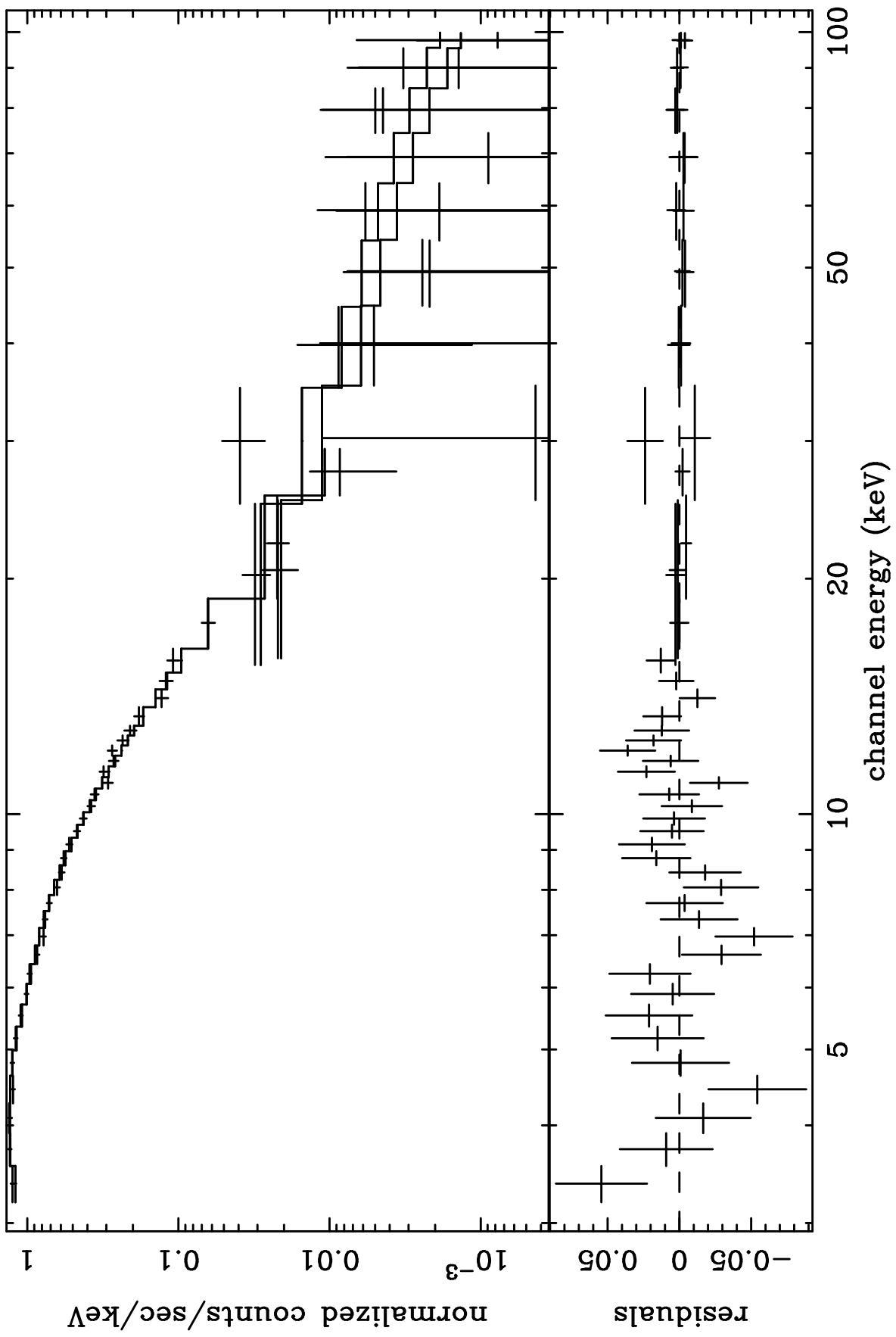


TABLE 2
RXTE OBSERVATIONS OF BL LACERTAE

Date (UT)	Time (h:m:s)	Observ. length (s)	Ct. rate & error	2-10 keV flux	Power law index & err	χ^2
PCA:						
16/07/97	00:58:56	1888	5.6 ± 0.2	2.0×10^{-11}	0.60 ± 0.10	24.9/45 PHA ch.
17/07/97	00:57:36	1936	7.0 ± 0.2	2.4×10^{-11}	0.57 ± 0.08	20.7/45 PHA ch.
18/07/97	18:48:00	1744	7.1 ± 0.2	2.4×10^{-11}	0.57 ± 0.10	30.7/45 PHA ch.
19/07/97	07:17:20	1728	11.0 ± 0.2	3.7×10^{-11}	0.43 ± 0.05	36.4/45 PHA ch.
20/07/97	13:54:08	1936	6.9 ± 0.2	2.5×10^{-11}	0.72 ± 0.09	27.5/45 PHA ch.
20/07/97	23:17:52	1968	9.5 ± 0.2	3.6×10^{-11}	0.81 ± 0.06	44.1/45 PHA ch.
21/07/97	23:15:28	1936	6.4 ± 0.2	2.2×10^{-11}	0.44 ± 0.08	26.4/45 PHA ch.
Full PCA data set		13136	7.6 ± 0.05	2.6×10^{-11}	0.59 ± 0.03	33.4/45 PHA ch.
HEXTE:						
Cluster A		4138	0.76 ± 0.22			
Cluster B		4077	0.33 ± 0.19			
Combined clusters A+B					$1.2^{+2.0}_{-0.8}$	136/158 PHA ch.
Combined PCA + HEXTE					0.59 ± 0.03	172/203 PHA ch.

NOTE.— All PCA counting rates are quoted over the 3 – 20 keV band. We quote the flux over the 2 – 10 keV band (in the units of $\text{erg cm}^{-2} \text{s}^{-1}$) for ease of comparison with previous observations. All HEXTE counting rates are over the 20 – 100 keV band.

NOTE.— Spectral fits to the PCA data were performed using a power law model over the channels nominally corresponding to the 3 – 20 keV band (45 PCA PHA channels), with the absorption fixed at the value measured by *Asca* ($2.7 \times 10^{21} \text{ cm}^{-2}$). In all cases, the absorption determined from the RXTE data was consistent with that determined from the *Asca* data; in all cases, the value of the fitted index did not vary by more than 0.03 when absorption was allowed to be free. For the HEXTE data, the fits were performed using channels corresponding to energy range 20 – 100 keV.

Comparison of the ROSAT PSPC, ASCA GIS, and RXTE PCA data on BL Lacertae

